

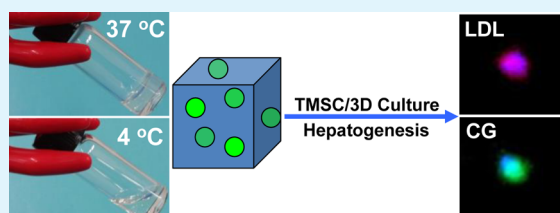
# Polypeptide Thermogels as a Three Dimensional Culture Scaffold for Hepatogenic Differentiation of Human Tonsil-Derived Mesenchymal Stem Cells

Seung-Jin Kim,<sup>†</sup> Min Hee Park,<sup>†</sup> Hyo Jung Moon, Jin Hye Park, Du Young Ko, and Byeongmoon Jeong\*

Department of Chemistry and Nano Science, Ewha Womans University, Global Top 5 Research Program, 52 Ewhayeodae-gil, Seodaemun-gu, Seoul, 120-750, Korea

## S Supporting Information

**ABSTRACT:** Tonsil-derived mesenchymal stem cells (TMSCs) were investigated for hepatogenic differentiation in the 3D matrices of poly(ethylene glycol)-*b*-poly(L-alanine) (PEG-L-PA) thermogel. The diblock polymer formed  $\beta$ -sheet based fibrous nanoassemblies in water, and the aqueous polymer solution undergoes sol-to-gel transition as the temperature increases in a concentration range of 5.0–8.0 wt %. The cell-encapsulated 3D matrix was prepared by increasing the temperature of the cell-suspended PEG-L-PA aqueous solution (6.0 wt %) to 37 °C. The gel modulus at 37 °C was about 1000 Pa, which was similar to that of decellularized liver tissue. Cell proliferation, changes in cell morphology, hepatogenic biomarker expressions, and hepatocyte-specific biofunctions were compared for the following 3D culture systems: TMSC-encapsulated thermogels in the absence of hepatogenic growth factors (protocol M), TMSC-encapsulated thermogels where hepatogenic growth factors were supplied from the medium (protocol MGF), and TMSC-encapsulated thermogels where hepatogenic growth factors were coencapsulated with TMSCs during the sol-to-gel transition (protocol GGF). The spherical morphology and size of the encapsulated cells were maintained in the M system during the 3D culture period of 28 days, whereas the cells changed their morphology and significant aggregation of cells was observed in the MGF and GGF systems. The hepatocyte-specific biomarker expressions and metabolic functions were negligible for the M system. However, hepatogenic genes of albumin, cytokeratin 18 (CK-18), and hepatocyte nuclear factor 4 $\alpha$  (HNF 4 $\alpha$ ) were significantly expressed in both MGF and GGF systems. In addition, production of albumin and  $\alpha$ -fetoprotein was also significantly observed in both MGF and GGF systems. The uptake of cardiogreen and low-density lipoprotein, typical metabolic functions of hepatocytes, was apparent for MGF and GGF. The above data indicate that the 3D culture system of PEG-L-PA thermogels provides cytocompatible microenvironments for hepatogenic differentiation of TMSCs. In particular, the successful results of the GGF system suggest that the PEG-L-PA thermogel can be a promising injectable tissue engineering system for liver tissue regeneration after optimizing the aqueous formulation of TMSCs, hepatogenic growth factors, and other biochemicals.



**KEYWORDS:** thermogel, hepatogenesis, TMSC, 3D culture, block copolymer

## 1. INTRODUCTION

Even though liver diseases are the major cause of morbidity and mortality, orthotopic liver transplantation is the only established method for the patients with acute liver failure or end-stage liver diseases.<sup>1,2</sup> However, lack of donor organs, surgical complications, immune rejection, and high costs remain as serious limitations associated with this procedure. Cell transplantation has emerged as an alternative treatment.<sup>3,4</sup> In this case, the difficulties related to collecting autologous liver tissues and maintaining the phenotype of the functional hepatocytes during cell culture need to be improved for the development of the cell-based therapy.<sup>5</sup> Therefore, the renewable supply of hepatocytes from other sources is a very important issue.

Stem cells have been highlighted as an alternative source of hepatocytes.<sup>6–8</sup> Mesenchymal stem cells (MSCs) have been investigated for cell-based hepatic therapies because they have

capability for multilineage differentiation, support the hematopoiesis, secrete proregenerative factors, and have immunological tolerance in the host tissues.<sup>9–11</sup> However, most of hepatogenic differentiation of MSCs has been studied on conventional two-dimensional (2D) cell culture systems which have intrinsic limitations in mimicking the 3D environments of living biological systems due to the differences in the cell–substrate contacts, cell–extracellular matrix interactions, and mass transports of nutrients and metabolites.<sup>12–14</sup> Such cellular microenvironments play a crucial role in directing the differentiation of the MSCs and maintaining the biofunctions of the hepatocytes. Therefore, development of differentiation protocols and optimizing culture conditions for MSCs in a

**Received:** July 16, 2014

**Accepted:** September 5, 2014

**Published:** September 5, 2014

cytocompatible 3D culture system is a very active area of research.

Recently, tonsil-derived MSCs (TMSCs) were reported as a new source of MSCs.<sup>15,16</sup> TMSCs not only have multilineage differentiation characteristics and immunosuppressive properties but also have easy availability from the surgery of tonsillar tissues.<sup>15</sup> Bone-marrow-derived MSCs (BMSCs) are still considered as a main source of MSCs; however, their number, proliferation rate, and differentiating potential have been shown to decrease with donor age. On the contrary, TMSCs are easily available from the tissues after tonsillectomy which is practiced mostly young persons, and thus above age-related complications are less serious than BMSCs. In particular, the tonsil tissues have been wasted after the surgery; therefore, the recovery of the stem cells from the waste tissues is also very important from the standpoint of recycling of the human tissues.

Thermogelling polymer aqueous solutions undergo sol-to-gel transition as the temperature increases. Because of their simple and biocompatible fabrication procedure to form an implant at a target site, they have been extensively investigated for drug delivery, tissue engineering, and other biomedical applications.<sup>17–23</sup> Thermogelling polymer systems do not use an organic solvent during the fabrication of the scaffold. In particular, the aqueous solution in a sol state can be filtered through membrane for sterilization, which significantly simplifies the fabrication process of the implant.<sup>24</sup> Instead of physical surgery, an implant or scaffold is formed by a simple syringe injection in a sol state, through the sol-to-gel transition of the system. In this study, we investigated the poly(ethylene glycol)-*b*-poly(L-alanine) (PEG-L-PA) thermogel as a potential 3D culture system of TMSCs to induce the differentiation of the stem cells into hepatocytes. The polypeptide based thermogel is degraded by mammalian enzymes such as elastases, and neutral pH is maintained during the degradation; thus, it provides a compatible environment for biopharmaceuticals and cells.<sup>25</sup> As a 3D culture system, growth factors and cells are coencapsulated as one pot. In the current study, we modulate the gel modulus to that of liver tissue for hepatogenic differentiation of the TMSCs. TMSCs were encapsulated in the PEG-L-PA thermogel by using sol-to-gel transition of the cell-suspended polymer aqueous solution. Three protocols were compared in this study. First, TMSCs were 3D cultured in the PEG-L-PA thermogel by using serum-free Iscove's modified Dulbecco's medium (IMDM) (protocol M). The protocol M was used as a control experiment for this study. Second, TMSCs were 3D cultured in the PEG-L-PA thermogel by using a hepatogenic medium containing growth factors such as hepatocyte growth factor (HGF), basic fibroblast growth factor (bFGF), epidermal growth factor (EGF), and oncostatin M. That is, the growth factors were supplied from the medium in a prescheduled manner as will be described in the materials and method section in detail (protocol MGF). Third, the total amount of above growth factors used in the MGF protocol was incorporated with TMSCs during the sol-to-gel transition of the PEG-L-PA aqueous solution, and the cells were 3D cultured by using IMDM. Therefore, the growth factors were supplied from the gel (protocol GGF). The last protocol, as it is, may be applied as an injectable tissue engineering of TMSCs for liver diseases. The gene expressions of albumin, cytokeratin 18 (CK-18), and hepatocyte nuclear factor 4 $\alpha$  (HNF4 $\alpha$ ) were compared for the three protocols to investigate the hepatogenic differentiation of the TMSCs under the above 3D culture

conditions. In addition, hepatocyte-specific functions such as the production of albumin and  $\alpha$ -fetoprotein as well as metabolic functions such as uptakes of cardiogreen (CG) and low-density lipoprotein (LDL) by the cells were assayed for the three protocols.

## 2. EXPERIMENTAL SECTION

**2.1. Materials.**  $\alpha$ -Amino- $\omega$ -methoxypoly(ethylene glycol)s (PEGs) ( $M_n = 1000$  Da) (ID Biochem Inc., Korea) and *N*-carboxyanhydrides of L-alanine (KPX Life Science, Korea) were used as received. Chloroform (Daejung, Korea) was treated with magnesium sulfate before use. A Live/Dead kit (Molecular Probes, USA), IQ SYBR Green Supermix (Bio-Rad, USA), and polymerase chain reaction (PCR) primers (Bioneer, Korea) were used as received. Toluene was dried over sodium before use.

**2.2. Synthesis of PEG-L-PA.** PEG-L-PA was synthesized by the ring opening polymerization of the *N*-carboxyanhydrides of L-alanine in the presence of  $\alpha$ -amino- $\omega$ -methoxy-PEG.<sup>26</sup> The  $\alpha$ -amino- $\omega$ -methoxy-PEG (2.5 g, 2.5 mmol; MW 1000 Da) was dissolved in anhydrous toluene (50 mL), and the residual water was removed by azeotropic distillation to a final volume of about 10 mL. Anhydrous chloroform/*N,N*-dimethylformide (30 mL, 2/1 v/v) and *N*-carboxyanhydrides of L-alanine (4.2 g, 36.5 mmol) were added to the reaction mixtures. They were stirred at 40 °C for 24 h under anhydrous nitrogen conditions. Polymers were purified by repeated dissolution in chloroform, filtration of an undissolved fraction, followed by precipitation into diethyl ether, and then evaporation of the residual solvent under vacuum. The polymer was dialyzed in water using a membrane with a cutoff molecular weight of 1000 Da and freeze-dried. The yield was about 65%.

**2.3. NMR Spectroscopy.** <sup>1</sup>H NMR spectra of the PEG-L-PA in CF<sub>3</sub>COOD were obtained by using the NMR spectrophotometer (500 MHz NMR spectrometer; Varian, USA) to determine the composition and number-average molecular weight ( $M_n$ ) of the polymers.

**2.4. Gel Permeation Chromatography.** A gel permeation chromatography system (SP930D, Younglin, Korea) with a refractive index detector (R1750F, Youglin, Korea) was used to obtain the molecular weights and molecular weight distributions of the polymers. An OHpak SB-802.5 HQ column (Shodex) was used. *N,N*-Dimethylformamide was used as an eluting solvent. PEGs with molecular weight in the range of 400–20 000 Da were used as molecular weight standards.

**2.5. Differential Scanning Calorimetry.** A differential scanning calorimeter (SINCO DSC N-650) was used to study the melting temperatures of the polymers in a temperature range of 0–300 °C with a heating and cooling rate of 5.0 °C/min. Polymer (about 5.0 mg) was loaded in a cell, and the thermogram was recorded during the second heating cycle.

**2.6. Cryotransmission Electron Microscopy.** Vitrified specimens of polymer aqueous solutions (0.06 wt %) were prepared on 200 mesh copper grids coated with a perforated form film (Ted Pella). A small drop (10  $\mu$ L) was applied to the grid at 15 °C and blotted with filter paper to form a thin liquid film of solution, which was immediately plunged into liquid ethane at –170 °C. The procedure was performed automatically in the Vitrobot. The vitrified specimens were imaged on a FEI Tecnai G2 TEM at 200 kV with a Gatan cryoholder maintained below –170 °C. Images were recorded on an Ultrascan 2K  $\times$  2K CCD camera. In the microscopes, images were recorded using the Digital Micrograph software package under low-dose conditions to minimize damage by the electron beam radiation.

**2.7. Dynamic Light Scattering.** The scattering intensity of the aqueous polymer solutions was studied by a dynamic light scattering instrument (ALV 5000-60x0) as a function of polymer concentration in a range of 0.001–0.5 wt % at 15 °C. A YAG DPSS-200 laser (Langen, Germany) operating at 532 nm was used as a light source. Measurements of the scattered light were made at an angle of 173° to the incident beam. The apparent size of PEG-L-PA aggregates in water was studied at 0.06 wt % by a dynamic light scattering instrument at 15 °C. The results of dynamic light scattering were analyzed by the

regularized CONTIN method. The decay rate distributions were transformed to an apparent diffusion coefficient. From the diffusion coefficient, the apparent hydrodynamic size of a polymer aggregate could be obtained by the Stokes–Einstein equation.

**2.8. Circular Dichroism Spectroscopy.** A circular dichroism spectrophotometer (J-810, JASCO) was used to study the ellipticity of the PEG-L-PA aqueous solution as a function of polymer concentration in a range of 0.01–0.10 wt % at 15 °C.

**2.9. FTIR Spectroscopy.** The FTIR spectrum (FTIR spectrophotometer FTS-800, Varian) of the PEG-L-PA aqueous solution (6.0 wt % in D<sub>2</sub>O) was investigated at 15 °C.

**2.10. Phase Diagram.** The sol–gel transition of the aqueous polymer solution was investigated by the test tube inverting method. The aqueous polymer solution (0.5 mL) was placed in a test tube with an inner diameter of 11 mm. The transition temperature was determined by the flow (sol)–no flow (gel) criterion by an increment of 1 °C per step. Each data point is an average of three measurements.

**2.11. Dynamic Mechanical Analysis.** Changes in modulus of the aqueous PEG-L-PA solution (6.0 wt %) that underwent sol-to-gel transition were investigated by dynamic rheometry (Rheometer RS 1; Thermo Haake, USA). The aqueous polymer solution was placed between parallel plates of 25 mm in diameter, with a gap of 0.5 mm. During the dynamic mechanical analysis, the samples were placed inside a chamber with water-soaked cotton to minimize the water evaporation. The moduli of the polymer aqueous systems were recorded under a controlled stress (4.0 dyn/cm<sup>2</sup>) with a frequency of 1.0 rad/s at 4 °C (sol) and 37 °C (gel).

**2.12. 3D Cell Culture.** TMSCs were isolated from the tonsils of a 16 year old male donor who had undergone tonsillectomy at the Ewha Womans University Mokdong Hospital (Seoul, Korea) following the ethical guidelines of the University. The isolated cells were monolayer cultured by using Dulbecco's modified Eagle medium (DMEM, Hyclone, USA) containing 10% fetal bovine serum (FBS, Hyclone, USA) and 1% penicillin/streptomycin (Hyclone, USA) under 5% CO<sub>2</sub> atmosphere at 37 °C. At 70–80% of confluence, cells were trypsinized. After confirmation of their characteristics as a MSC by showing the negative expressions of hematopoietic stem cell biomarkers of CD14, CD34, and CD45 but positive expressions of mesenchymal stem cell biomarkers for CD73, CD90, and CD105, they were used for subsequent experiments (Supporting Information, Figure S1).<sup>15</sup> Three protocols were compared in this study.

**Protocol M.** Passage-six cells were mixed with an aqueous polymer solution of serum-free Iscove's modified Dulbecco's medium (IMDM, Hyclone, USA) (6.0 wt %, 0.2 mL) with a density of 2.0 × 10<sup>6</sup> cells/mL. Temperature of the TMSC-suspended aqueous system increased to 37 °C to form a cell-embedded 3D matrix. Then the serum-free IMDM was replaced every 3 days during the 3D culture period of 28 days.

**Protocol MGF.** Passage-six cells were mixed with an aqueous polymer solution of serum-free IMDM (6.0 wt %, 0.2 mL) with a density of 2.0 × 10<sup>6</sup> cells/mL. Temperature of the TMSC-suspended aqueous system increased to 37 °C to form a cell-embedded 3D matrix. Hepatogenic differentiation of TMSCs was performed as described previously with minor modifications.<sup>27–29</sup> First, the cells were serum-deprived for 2 days in IMDM supplemented with 20 ng/mL epidermal growth factor (EGF, Peprotech, USA) and 10 ng/mL basic fibroblast growth factor (bFGF, Peprotech, USA). Then the medium was changed to serum-free IMDM containing 20 ng/mL hepatocyte growth factor (HGF, Peprotech, USA), 10 ng/mL bFGF, and 0.61 g/L nicotinamide (Sigma, USA). The medium was replaced every 3 days for 12 days to generate hepatocytes. For hepatic maturation, IMDM was subsequently supplemented with 20 ng/mL oncostatin M (Sigma, USA), 1 M dexamethasone (Sigma, USA), and 50 mg/mL ITS+ (Sigma, USA), and the medium was replaced every 3 days for another 14 days.

**Protocol GGF.** Total amount of growth factors used in the protocol MGF was incorporated into the gel with TMSCs during the sol-to-gel transition. Then serum-free IMDM was replaced every 3 days for 28 days.

For all three protocols of M, MGF, and GGF, the encapsulated cells in the PEG-L-PA thermogel were 3D cultured under 5% CO<sub>2</sub> atmosphere at 37 °C.

**2.13. Cell Proliferation.** Proliferation of TMSCs in the PEG-L-PA thermogel was assessed by the CCK-8 methods (*n* = 3). CCK-8 solution (1.5 mL, 10% v/v in medium) was added to each well of the plate. After 3 h of incubation, the absorbance at 450 nm was measured with an ELISA reader (model 550; Bio-Rad, Hercules, CA, USA), where the absorbance at 655 nm was used as a baseline. Viability and morphology of TMSCs in the PEG-L-PA thermogel was determined using the Live/Dead kit (Molecular Probes, Life Technologies, USA). Samples were incubated at room temperature for 30 min in a solution of 4.0 M ethidium homodimer-1 (EthD-1) and 2.0 M calcein AM in phosphate buffered saline. Labeled cells were then viewed under an Olympus IX71 fluorescence microscope, and images were captured using the Olympus DP2-BSW software. Live cells were stained with calcein AM (green), whereas dead cells were stained with EthD-1 (red).

**2.14. RNA Extraction and Real-Time Reverse Transcription Polymerase Chain Reaction.** The TRIzol reagent (Invitrogen, Canada) was used to extract the total mRNA from the cell-encapsulated hydrogels after 0, 7, 14, 21, and 28 days of 3D culture according to the manufacturer's protocol. The extracted mRNA pellet was dissolved in nuclease-free water, and the mRNA concentration was determined using a Nano Drop (ND-1000) spectrophotometer (Thermo Scientific, USA). After synthesis of the cDNA from the isolated mRNA, cDNA samples were stored at –20 °C until needed. Real-time RT-PCR was performed using the Rever Tra Ace qPCR RT kit (Toyobo, Japan). The PCR procedure consisted of an initial denaturation at 95 °C for 3 min, followed by 40 cycles of denaturation at 95 °C for 15 s and annealing and extension at 65 °C for 30 s. The PCR products were visualized by the SYBR green. The primers used for amplification are listed in Table 1. Relative expression level of

**Table 1. Primer Sequences and PCR Conditions for Real-Time RT-PCR<sup>a</sup>**

target gene	primer sequence
albumin	F: 5'-GATGTCTTCCTGGCA-3' R: 5'-CTTGGGCTTGTGTTTCAC-3'
HNF4 $\alpha$	F: 5'-ATCGTCAAGCCCTCTCTG-3' R: 5'-TCTTCCCTTTCGGTGACC-3'
CK-18	F: 5'-GAAGGAGACCATGCAAAGCCTG-3' R: 5'-CATGAAGAGCAGCTCCTCCTTG-3'
GAPDH	F: 5'-ATGGGGAAGGTGAAGGTCG-3' R: 5'-TAAAGCAGCCCTGGTGACC-3'

<sup>a</sup>HNF4 $\alpha$ , CK-18, and GAPDH indicate hepatocyte nuclear factor 4 $\alpha$ , cytokeratin 18, and glyceraldehyde 3-phosphate dehydrogenase, respectively. F and R indicate forward and reverse primers, respectively. Annealing temperature is 57 °C.

target genes was calculated as 2<sup>– $\Delta\Delta C_t$</sup> , where target gene expression was normalized as  $\Delta\Delta C_t = (\text{gene A} - \text{GAPDH})_T - (\text{gene A} - \text{GAPDH})_{T_0}$ . T<sub>0</sub> is the data on the day when the experiment started.

**2.15. Protein Production.** At the designated time points, the conditioned media of the differentiated TMSCs in each system of M, MGF, and GGF were collected and frozen at –80 °C until used for assaying. Albumin and  $\alpha$ -fetoprotein ELISA kits (Abcam, U.K.) were used according to the manufacturer's protocol. Albumin and  $\alpha$ -fetoprotein production were determined using the ELISA reader (Bio-Rad, USA) at 450 nm.

**2.16. Metabolic Function.** The CG uptake was assayed as previously described.<sup>30</sup> CG (Sigma, USA) was dissolved in sterile 0.01 M phosphate buffered saline to produce a fresh CG solution at 5.0 mg/mL and was diluted in IMDM to a final concentration of 1.0 mg/mL. The 3D cultured TMSCs were incubated for 28 days with the CG solution for 30 min at 37 °C.

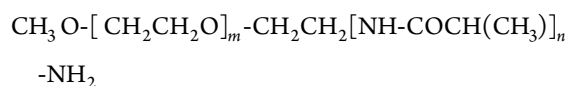
For the LDL uptake assay, the Dil-Ac-LDL staining kit (Invitrogen, USA) was used in accordance with the manufacturer's protocols. The 3D cultured TMSCs were incubated with 20  $\mu\text{g}/\text{mL}$  Dil-Ac-LDL for 3 h at 37  $^{\circ}\text{C}$ . The 3D cultured cells were washed by phosphate buffered saline three times before the nuclei were counterstained by NucBlue (Life Technologies, USA).

The images were examined using an Olympus IX71 fluorescence microscope and were captured using the Olympus DP2-BSW software.

**2.17. Statistical Analysis.** The data were expressed as the mean  $\pm$  standard error of the mean (SEM). The differences in the mean values were evaluated using the one-way ANOVA with Tukey tests. Differences were considered significant when the  $p$  value was less than 0.05 (marked as \*\*).

### 3. RESULTS

PEG-L-PA was synthesized by the ring-opening polymerization of *N*-carboxyanhydrides of L-alanine in the presence of  $\alpha$ -amino- $\omega$ -methoxy-PEG. The basic characteristics of the polymer in a bulk state were studied by  $^1\text{H}$  NMR spectroscopy, gel permeation chromatography, and differential scanning calorimetry. The molecular weight of the PEG-L-PA was determined by comparing the methyl peak of L-alanine ( $-\text{NHCH}(\text{CH}_3)\text{CO}-$ ) at 1.4–1.9 ppm and the ethylene glycol ( $-\text{CH}_2\text{CH}_2\text{O}-$ ) peak of PEG at 3.8–4.2 ppm in the  $^1\text{H}$  NMR spectrum of PEG-L-PA ( $\text{CF}_3\text{COOD}$ ) (Figure 1a).



$$A_{1.4-1.9}/A_{3.8-4.2} = 3n/(4m + 2)$$

Assuming  $m$  being 22.7 for the PEG with a molecular weight of 1000 Da, the degree of polymerization of L-PA determined by  $^1\text{H}$  NMR spectra is 11.2. Therefore, the number-average molecular weight ( $M_n$ ) of each block of the PEG-L-PA is 1000–795. The gel permeation chromatogram of the PEG-L-PA showed unimodal distribution of the molecular weights with a polydispersity index ( $M_w/M_n$ ) of 1.2, and the number-average molecular weight ( $M_n$ ) and weight-average molecular weight ( $M_w$ ) determined against PEG standards are 1100 and 1320, respectively (Figure 1b).

Differential scanning calorimetry thermogram of the bulk PEG-L-PA exhibited two melting peaks at 15–40  $^{\circ}\text{C}$  (peak at 31  $^{\circ}\text{C}$ ) and 180–220  $^{\circ}\text{C}$  (peak at 213  $^{\circ}\text{C}$ ), which correspond to the melting transition of PEG and L-PA, respectively (Figure 1c). The independent melting peaks are the typical behavior of a block copolymer with immiscible blocks.<sup>31</sup>

The self-assembly of the PEG-L-PA in water was investigated by cryotransmission electron microscopy, dynamic light scattering, circular dichroism spectroscopy, and FTIR spectroscopy. The cryotransmission electron microscopy image of aqueous polymer solution was developed from the 0.06 wt % PEG-L-PA in water. The nanofibrillar structure with few hundreds nanometer in length was observed (Figure 2a).

The critical aggregation concentration (CAC) of amphiphilic molecules has been reported by using various techniques such as surface tension, conductivity, UV–vis spectroscopy, and fluorescence measurements.<sup>32–35</sup> Dynamic light scattering, another popular method for the determination of CAC, was used for the current study.<sup>36,37</sup> Below the CAC, the intensity of scattered light of a solution is similar to that obtained from water. However, above the CAC, the intensity of scattered light significantly increases due to the presence of aggregates. As the concentration of the PEG-L-PA increased over 0.001–0.5 wt %, the

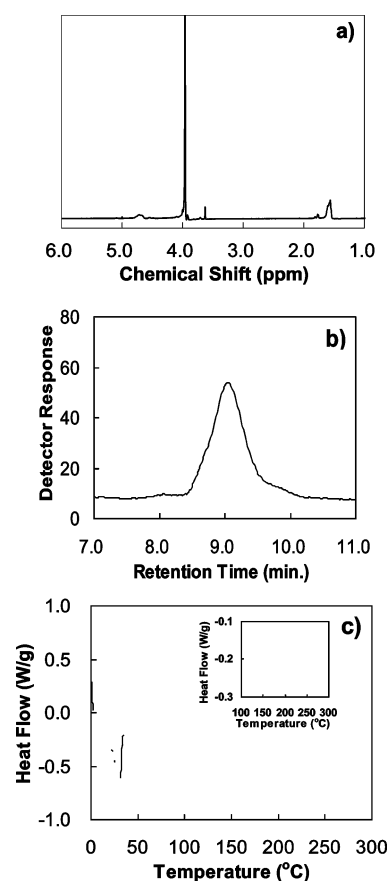


**Figure 1.** Basic characteristics of PEG-L-PA: (a)  $^1\text{H}$  NMR spectra ( $\text{CF}_3\text{COOD}$ ); (b) gel permeation chromatogram (*N,N*-dimethylformamide); (c) differential scanning calorimetric thermogram.

the scattering intensity of the polymer aqueous solution abruptly increased in the concentration range of 0.01–0.05 wt %, suggesting that the aggregates began to form in this concentration range (Figure 2b). CAC was determined to be in a range of 0.01–0.05 wt %. Dynamic light scattering study of the aqueous polymer solution was studied at 0.06 wt % which is above the CAC. The data exhibited the nanoassembled structures of 30–350 nm in size with a peak average size of 105 nm (Figure 2c). From the dynamic light scattering study and cryo-TEM images, we can conclude that the block copolymers of PEG-L-PA form fibrous self-assemblies with a broad distribution of 30–350 nm in size.

Circular dichroism spectra exhibited a negative Cotton band centered at 218 nm, suggesting that the PEG-L-PAs formed a well-defined  $\beta$ -sheet structure in water (Figure 2d).<sup>38,39</sup> The cryotransmission electron microscopy and circular dichroism spectra suggested that the  $\beta$ -sheet-based nanoassemblies with hundred nanometers in size were responsible for the increase in scattering intensity in dynamic light scattering study. The  $\beta$ -sheet-based self-assemblies were also preserved in a high concentration range of 6.0 wt % that exhibited sol-to-gel transition, as shown by the peak at 1626  $\text{cm}^{-1}$  in the FTIR spectra of PEG-L-PA aqueous solution in  $\text{D}_2\text{O}$  (Figure 2e).<sup>38,39</sup>

PEG-L-PA aqueous solutions underwent sol-to-gel transition as the temperature increased. The gelation mechanism of the PEG-L-PA has been reported by our group.<sup>26</sup> Briefly, the dehydration of the PEG and aggregation of the  $\beta$ -sheeted nanoassemblies accompanying a partial strengthening of the  $\beta$ -sheet structure occurs as the temperature increases.

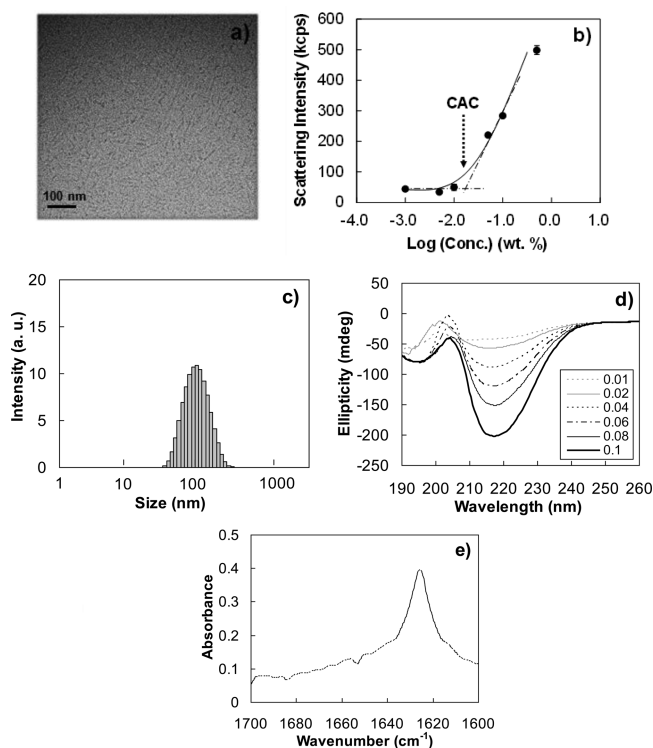


**Figure 2.** Self-assembly of PEG-L-PA in water: (a) cryotransmission electron microscopy image developed from the aqueous PEG-L-PA solution (0.06 wt %); (b) critical aggregation concentration (CAC) determined by dynamic light scattering at 15 °C; (c) size distribution of PEG-L-PA nanoassemblies in water at 0.06 wt %; (d) circular dichroism spectra of aqueous PEG-L-PA solution as a function of concentration at 15 °C; (e) FTIR spectra of aqueous PEG-L-PA solution (6.0 wt % in D<sub>2</sub>O) at 15 °C.

The phase diagram of sol-to-gel transition was constructed by the test tube inverting method based on the flow (sol)–no flow (gel) criterion when the vial was inverted. The transition temperature was reproducible because of the large difference (more than 1000 times) in viscosity or modulus between sol and gel states. The sol-to-gel transition temperature of the aqueous polymer solution decreased from 22 ( $\pm 1.1$ ) to 7 ( $\pm 1.5$ ) °C as the concentration increased from 5.0 to 8.0 wt % (Figure 3a). At concentrations below 5.0 wt %, the aqueous polymer solution increased its viscosity as the temperature increased. However, the system was still in a flow state when the vial was inverted; therefore, it was defined as a sol. On the other hand, at concentrations greater than 8.0 wt %, the aqueous polymer system was a gel over the investigated temperature range of 4–50 °C.

The polymer concentration selected for dynamic mechanical analysis was 6.0 wt %. Dynamic mechanical analysis was carried out in the sol (4 °C) and gel (37 °C) states. The gel modulus at 37 °C was about 700–1000 Pa, whereas the modulus was less than 0.5 Pa in a sol state at 4 °C (Figure 3b). On the basis of the fact that the modulus of the decellularized liver tissue is about 0.9–1.2 kPa, we selected a gel system with a modulus of about 1 kPa at 37 °C for the 3D culture of TMSC for hepatogenic differentiation.<sup>40</sup>

Photos in the sol (4 °C) and gel (37 °C) states of the polymer aqueous solution (6.0 wt %) were also included in Figure 3b.

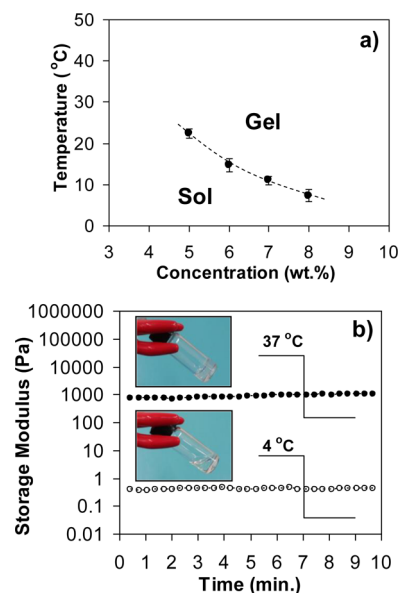


**Figure 3.** (a) Phase diagram of PEG-L-PA aqueous solutions. The transition temperature was determined by the test tube inverting method. (b) Changes in the modulus of PEG-L-PA aqueous solution (6.0 wt %) as a function of temperature. The photos of a sol state at 4 °C and a gel state at 37 °C are inserted.

The cell renewal and differentiation are affected by cellular microenvironments such as spatial distributions of hormones and growth factors as well as cell–matrix interactions. However, it is difficult to achieve biomimetic microenvironments under traditional 2D culture systems.<sup>12–14,41</sup> In this study, PEG-L-PA thermogels were used as a 3D culture system, and differentiation of TMSCs into hepatocytes was investigated. To establish the 3D cell culture systems, temperature of the TMSC-suspended PEG-L-PA aqueous solution increased to the cell culture temperature of 37 °C. The temperature-sensitive sol-to-gel transition of the system produced a 3D matrix for TMSCs. The TMSCs were 3D cultured by the protocols of M, MGF, and GGF, as described in the materials and methods section in detail. PEG-L-PA thermogel systems of M, MGF, and GGF maintained their overall three-dimensional integrity without significant mass loss over the cell culture period of 28 days. Proliferation and viability of the encapsulated cells were evaluated by the CCK-8 method for M, GGF, and MGF systems. The cell proliferation of the TMSCs as measured by optical density at 450 nm was similar for the three systems except for the 28th day, when the optical density was higher ( $p < 0.05$  by ANOVA analysis) in the MGF system than the M or the GGF system (Figure 4a). The cells in the M system maintained their spherical morphology with 10  $\mu\text{m}$  in size over 28 days, whereas the cells in the GGF and MGF systems showed stretched or aggregated morphologies of the cells with a size of 20–30  $\mu\text{m}$  (Figure 4b and Figure 4c). Under the 2D culture conditions, the cell morphologies of various MSCs derived from placenta, adipose tissue, bone marrow, and umbilical cord blood did not change during the initiation step of hepatogenic differentiation, except the fibroblastic morphology was lost and cells developed a broadened flattened shape.<sup>27,42</sup> In a 3D hydrogel system, however, spherical embryoid bodies of aggregates were formed during hepatogenic differentiation of murine embryonic stem cells (mESCs) and murine induced pluripotent stem cells (miPSs).<sup>43</sup> Our result also indicated that cell morphology considerably changed and

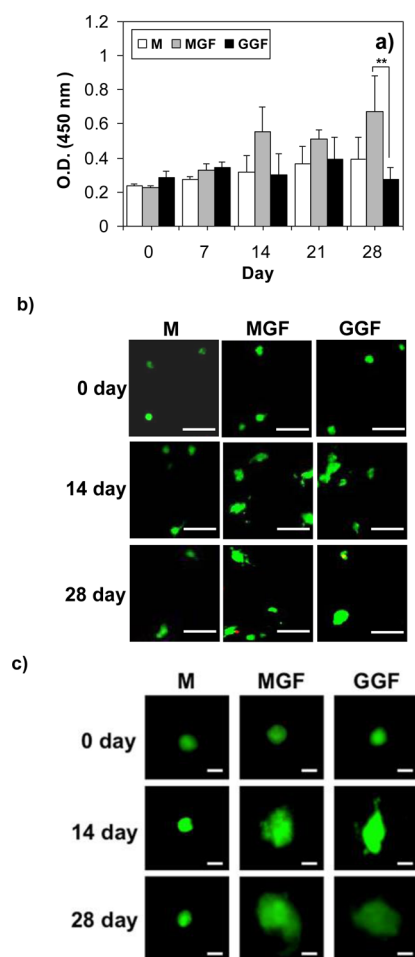


**Figure 4.** (a) Changes in optical density (OD) at 450 nm of the TMSCs in the PEG-L-PA thermogels analyzed by CCK-8. The data are the mean  $\pm$  SEM for triplicate experiments. (b) Changes in morphologies of 3D cultured TMSCs in the PEG-L-PA thermogels. The scale bar is 50  $\mu$ m. (c) Enlarged images of the cells. The scale bar is 10  $\mu$ m. Shown are TMSCs cultured in the in situ formed PEG-L-PA hydrogel in the absence of hepatogenic growth factors (M), in the presence of hepatogenic growth factors supplied in the medium (MGF), and in the presence of hepatogenic growth factors coencapsulated with the cells in the hydrogel (GGF).

cell aggregates formed in the PEG-L-PA thermogels in the presence of hepatogenic growth factors.

mRNA expressions for hepatogenesis were also compared for three protocols of M, MGF, and GGF. The total mRNA extracts from the cell-encapsulated hydrogels were analyzed for the hepatogenic biomarkers of albumin, CK-18, and HNF4 $\alpha$  using real-time RT-PCR. Albumin is an early fetal and mature hepatocyte differentiation biomarker, and CK-18 is the major intermediate filament protein in the liver.<sup>44,45</sup> HNF4 $\alpha$  is a transcription factor that regulates liver genes, and thus the presence of HNF4 $\alpha$  implies the progression of hepatogenesis during early embryogenesis.<sup>18,39</sup> All of them are key biomarkers for hepatogenic differentiation from the stem cells.<sup>27,28,42,43</sup>

Compared with the M system, all of the above hepatogenic biomarkers were highly expressed in both MGF and GGF systems where the hepatogenic growth factors were supplied. Practically, there is negligible expression of hepatogenic biomarkers in the M system, suggesting that the hepatogenic growth factors are critical for hepatogenic differentiation of the TMSCs. In particular, mRNAs of albumin and HNF4 $\alpha$  were

more significantly expressed in the MGF system than the GGF system, whereas those of CK-18 were also highly expressed in both MGF and GGF systems (Figure 5a and Figure 5b). The

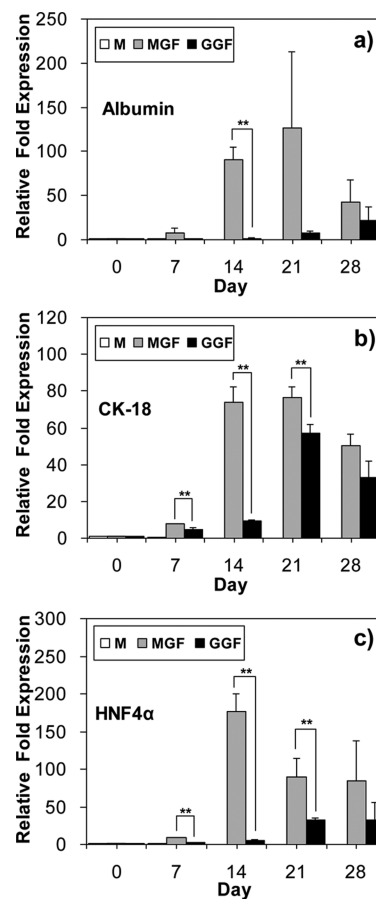


**Figure 5.** (a) mRNA expressions for albumin, (b) CK-18, and (c) HNF4 $\alpha$  of 3D cultured TMSCs in the PEG-L-PA thermogels. The samples were analyzed by real-time RT-PCR. The data were normalized by the GAPDH and 0th day data. The data are presented as the mean  $\pm$  SEM of triplicate experiments (mean  $\pm$  SEM,  $n = 3$ ; ANOVA (\*\*))  $p < 0.05$ .

albumin and CK-18 were up-regulated in a time-dependent manner until the 21st day and was slightly down-regulated on the 28th day of the MGF protocol. The HNF4 $\alpha$  was up-regulated until the 14th day and was slightly down-regulated after the 21st day in the MGF system (Figure 5c). On the other hand, both albumin and HNF4 $\alpha$  were up-regulated until the 28th day in the GGF system. Previous studies demonstrated that expression patterns of hepatogenic biomarkers such as HNF3 $\beta$ ,  $\alpha$ -fetoprotein, transthyretin, HNF1 $\alpha$ , HNF4 $\alpha$ , albumin, CK-18, tryptophan 2,3-dioxygenase, and tyrosine amino transferase were time-dependently up-regulated in 2D and 3D stem cell culture systems. Some studies showed respective temporal expression patterns during the hepatogenic differentiation event, suggesting that patterns of the biomarker expressions for hepatogenic differentiation can be affected by culture environments (2D or 3D), differentiation factors, and type of MSCs.<sup>28,43,38–50</sup> Our 3D culture system of PEG-L-PA thermogel has proven to be effective in inducing the hepatogenic differentiation of TMSCs as demonstrated by the typical hepatogenic biomarker expressions.

Production of albumin and  $\alpha$ -fetoprotein is the main characteristic of mature hepatocytes. Therefore, the presence of the biomarkers can be considered definitive evidence of hepatogenic differentiation of the stem cells. The above biomarkers collected from the culture media were compared for the three protocols of M, MGF, and GGF after 14, 21, 28 days of incubation. Production of albumin and  $\alpha$ -fetoprotein was not detected in the M system, where the TMSCs were 3D cultured in the absence of hepatogenic growth factors. In the presence of the hepatogenic growth factors, albumin production increased in both GGF and MGF systems, with higher ( $p < 0.05$  by ANOVA analysis) production in the MGF system than the GGF system over 21–28 days (Figure 6a).

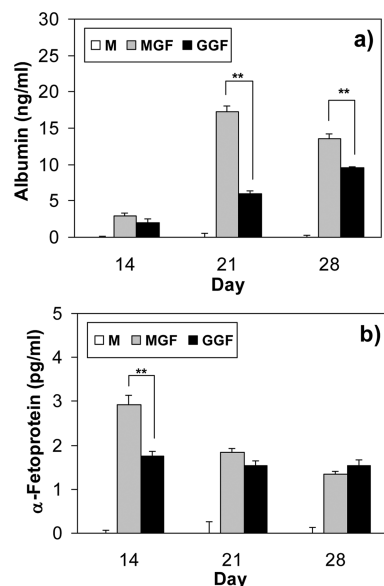


**Figure 6.** Protein production for albumin (a) and  $\alpha$ -fetoprotein (b) of the 3D cultured TMSCs in the PEG-L-PA thermogels (mean  $\pm$  SEM,  $n = 3$ ; ANOVA (\*\*))  $p < 0.05$ ).

Production of  $\alpha$ -fetoprotein was also higher ( $p < 0.05$  by ANOVA) in the MGF system than the GGF system for 14 days of incubation; however, both MGF and GGF systems exhibited a similar  $\alpha$ -fetoprotein production over 21–28 days (Figure 6b). Previous studies demonstrated that production of albumin and  $\alpha$ -fetoprotein increased with time during differentiation or maturation periods of stem cell hepatogenesis, and their production in 3D cell culture systems was similar to or better than 2D culture system.<sup>28,42,43,51</sup> Our results again indicated the successful hepatogenesis of TMSCs in the PEG-L-PA thermogel in the presence of the hepatogenic growth factors as in the MGF and GGF systems.

In order to determine liver-specific metabolic functions of the differentiated hepatocytes, uptakes of CG and LDL were investigated (Figure 7a and Figure 7b). CG is a clinically used organic anion to examine the hepatic function and is specifically taken up by hepatocytes, whereas LDL is also taken up and metabolized by hepatocytes.<sup>30,52</sup> The CG and LDL exhibited as green and red, respectively, only after their uptakes into the hepatocytes. Nuclei of the cells were stained in blue by 4',6-diamidino-2-phenylindole (DAPI). The merged images show an uptake of the CG and LDL into the cells in both GGF and MGF systems, whereas the uptake was not observed for the cells in the M system. These results also indicate that the

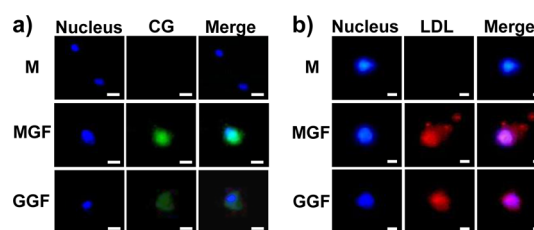


**Figure 7.** Cellular uptake of (a) CG and (b) LDL by the 3D cultured TMSCs for 28 days in the PEG-L-PA thermogels. The scale bar is 10  $\mu$ m.

TMSCs cultured in PEG-L-PA thermogels differentiated into hepatocytes in the presence of growth factors (MGF and GGF systems).

#### 4. DISCUSSION

PEG and L-PA are immiscible blocks in a bulk system, and they form a core-shell structure in water due to the hydrophilic and hydrophobic nature of the PEG and L-PA, respectively. PEG-L-PA self-assembled into  $\beta$ -sheets in water, and then they assembled into nanostructures with more than 100 nm in size. TMSCs were encapsulated in the 3D culture systems of PEG-L-PA thermogels by increasing temperature of the cell-suspended aqueous polymer solutions. The 6.0 wt % of the aqueous polymer solution was selected to provide the modulus of 1 kPa at 37  $^{\circ}$ C, which is the modulus of decellularized normal liver tissue.<sup>40</sup> The TMSCs expressed liver-specific mRNAs in the presence of hepatogenic growth factors, suggesting that the stem cells successfully differentiated into hepatocytes during the 3D culture. Albumin, a mature hepatocyte differentiation biomarker, was similarly expressed in both MGF and GGF systems on the 14th day but significantly more expressed in the MGF system than the GGF system on days 21–28. Both CK-18 (a major intermediate filament protein in the liver) and HNF4 $\alpha$  (a transcription factor that regulates liver genes) were also more expressed in the MGF system than the GGF system over 7–21 days; however, it was expressed in a similar extent on the 28th day in both MGF and GGF systems. Ideally, the growth factors should be provided according to the cell cycle, where each growth factor plays roles in each step of cell differentiation. When the local concentration of the growth factors is too high at an inappropriate time, it may give negative effects on the biomarker expressions. The protocol MGF has more advantages than GGF in this regard because the growth factors were replaced every 3 days in a prescheduled manner and different combinations of growth factors were used in the hepatogenic differentiation stage for the first 12 days and the hepatic maturation stage for the last 14 days. However, the growth factors were coencapsulated with the TMSCs in the GGF system, and they should diffuse through the hydrogel to reach nearby cells or diffuse into the medium which was discarded during the medium replacement. Therefore, the differences in biomarker expressions between MGF and GGF systems might be related to the difference in the availability of the growth factors to the cells.

To confirm the existence of mature hepatocytes, hepatocyte-specific biofunctions and metabolic functions were assayed. A significant amount of albumin and  $\alpha$ -fetoprotein production was detected from 3D culture systems of TMSCs in the presence of hepatogenic growth factors (both MGF and GGF systems) over days 14–28. In addition, hepatocyte-specific

metabolic functions such as CG and LDL uptakes were also observed for both MGF and GGF systems.

Albumin secretion as a measure of the hepatogenic differentiation can be compared among several systems by normalizing the number of cells. The mouse embryonic stem cells (ESCs) were cultured for 20 days toward hepatogenic differentiation in a 3D scaffold of poly(lactic-co-glycolic acid) nanofiber matrix.<sup>30</sup> The system secreted albumin  $1100 \text{ pg mL}^{-1} \text{ day}^{-1}$  ( $10^5 \text{ cells}^{-1}$ ). The induced pluripotent stem cells (iPSs) of mice were cultured for hepatogenic differentiation on a gelatin coated plate for 16 days.<sup>53</sup> The albumin secretion was measured to be  $396 \text{ pg mL}^{-1} \text{ day}^{-1}$  ( $10^5 \text{ cells}^{-1}$ ). Murine iPSs and ESCs were 3D cultured in alginate microporous hydrogels for 30 days.<sup>51</sup> Albumin was secreted about  $3000\text{--}5000 \text{ pg mL}^{-1} \text{ day}^{-1}$  ( $10^5 \text{ cells}^{-1}$ ) for the both systems. A 2D cultured system secreted a similar amount of albumin for ESCs, whereas about half of the albumin was secreted for iPSs. In our hepatogenic differentiation systems of TMSCs by using the PEG-L-PA as a 3D culture system, the cells cultured for 28 days secreted  $10\text{--}15 \text{ ng mL}^{-1}$  ( $4 \times 10^5 \text{ cells}^{-1}$ ), corresponding to  $2500\text{--}3750 \text{ pg mL}^{-1} \text{ day}^{-1}$  ( $10^5 \text{ cells}^{-1}$ ).

mRNA expressions, protein production, and metabolic functions of 3D cultured TMSCs in the PEG-L-PA thermogels consistently indicated the successful hepatogenic differentiation of TMSCs in the presence of the hepatogenic growth factors. Biomarkers of albumin, CK-18, and HNF4a were similar or better for the MGF system than the GGF system under the 3D in vitro culture conditions. During the in vitro cell culture period, the growth factors and nutrients can be externally modulated by replacing the culture medium. When it comes to in vivo application of the system for injectable tissue engineering, the growth factors and nutrients cannot be modulated externally. In this regards, the GGF protocol has the potential for an injectable tissue engineering application by injecting an aqueous polymer solution containing both growth factors and TMSCs to a target site of the liver.

Although hepatogenic differentiation has recently been achieved in 3D cultures using embryonic stem cells (ESCs),<sup>30,52,54–56</sup> the research associated with hepatogenic differentiation of MSCs in 3D culture system is rarely reported.<sup>56–58</sup> Cytokines and growth factors such as HGF, EGF, transforming growth factor (TGF), bFGF, insulin, insulin-like growth factor, and oncostatin M were reported to affect the hepatogenic differentiation of the stem cells.<sup>1,51–56</sup> bFGF initiates early liver development in the foregut endoderm, and HGF stimulates hepatoblast proliferation.<sup>1</sup> Oncostatin M is produced by hematopoietic stem cell during the early stage of embryogenesis and induces fetal hepatogenic differentiation and maturation.<sup>51</sup> Insulin–transferrin–selenium premix (ITS+) promotes the proliferation and survival of primary hepatocytes.<sup>51</sup> Recent studies demonstrate that activin A and sequential addition of growth factors and hormones promoted induced pluripotent stem cells (iPS) into hepatocytes in a 3D hydrogel system.<sup>43,59</sup> In addition, chemical compounds such as dexamethasone, retinoic acid, sodium butyrate, nicotinamide, norepinephrine, and dimethyl sulfoxide are known to induce hepatogenic differentiation.<sup>48,51,60,61</sup> Nicotinamide induces the proliferation of hepatocytes and formation of small hepatocytes colonies.<sup>46</sup> Dexamethasone induces the expression of liver-enriched transcription factors such as HNF4 and the enhancer-binding protein  $\alpha$  (EBP $\alpha$ ), which are important transcription factors for hepatocyte differentiation.<sup>46</sup>

Current study proved the feasibility of PEG-L-PA as a 3D culture system of TMSCs for hepatogenic differentiation. However, the above biological and chemical factors should be optimized for further study considering the injectable tissue engineering application of the current system.

## 5. CONCLUSIONS

We investigated PEG-L-PA thermogelling system that undergoes sol-to-gel transition in response to temperature changes. The 3D matrix can be formed by simply increasing the temperature of a cell-suspended polymer aqueous solution to  $37^\circ\text{C}$  without chemical reaction or using organic solvents. Therefore, a 3D cell growing matrix can be formed in vivo by syringe injection to a target site of warm-blood animals or human without surgical procedure. In particular, the GGF protocol holds the potential for an injectable tissue engineering application by injecting the aqueous polymer solution containing growth factors and TMSCs to a target site of the liver for tissue regeneration. However, the combination of growth factors, cytokines, or chemicals should be carefully selected to maximize the hepatogenic differentiation of the stem cells. Therefore, further studies are needed to optimize the current thermogel as a 3D culture system of TMSCs. In addition, in vivo studies are also needed to confirm efficiency of cell therapy and biocompatibility of the TMSC/PEG-L-PA thermogel.

The current study is significant in that a TMSCs/PEG-L-PA/growth factor system is a promising 3D system for the differentiation of TMSCs into functional hepatocytes.

## ■ ASSOCIATED CONTENT

### 📄 Supporting Information

Surface marker expressions of TMSCs by flow cytometry. This material is available free of charge via the Internet at <http://pubs.acs.org>.

## ■ AUTHOR INFORMATION

### Corresponding Author

\*E-mail: [bjeong@ewha.ac.kr](mailto:bjeong@ewha.ac.kr). Phone: +82 2 3277 3411. Fax: +82 2 3277 2384.

### Author Contributions

†S.-J.K. and M.H.P. equally contributed to the paper.

### Notes

The authors declare no competing financial interest.

## ■ ACKNOWLEDGMENTS

This work was supported by the National Research Foundation of Korea Grant funded by the Korean Government (Grant MSIP 2012M3A9C6049835). S.-J.K. was supported by RP-Grant 2013 of Ewha Womans University.

## ■ REFERENCES

- (1) Lee, H. J.; Jung, J.; Cho, K. J.; Lee, C. K.; Hwang, S. G.; Kim, G. J. Comparison of in Vitro Hepatogenic Differentiation Potential between Various Placenta-Derived Stem Cells and Other Adult Stem Cells as an Alternative Source of Functional Hepatocytes. *Differentiation* **2012**, *84*, 223–231.
- (2) Keeffe, E. B. Liver Transplantation: Current Status and Novel Approaches to Liver Replacement. *Gastroenterology* **2001**, *120*, 749–762.
- (3) Nussler, A.; Konig, S.; Ott, M.; Sokal, E.; Christ, B.; Thasler, W.; Brulport, M.; Gabelein, G.; Schormann, W.; Schulze, M.; Ellis, E.; Kraemer, M.; Nocken, F.; Fleig, W.; Manns, M.; Strom, S. C.;



Hengstler, J. G. Present Status and Perspectives of Cell-Based Therapies for Liver Diseases. *J. Hepatol.* **2006**, *45*, 144–159.

(4) Vosough, M.; Moslem, M.; Pournasr, B.; Baharvand, H. Cell-Based Therapeutics for Liver Disorders. *Br. Med. Bull.* **2011**, *100*, 157–172.

(5) Zamule, S. M.; Coslo, D. M.; Chen, F. M.; Omiecinski, C. J. Differentiation of Human Embryonic Stem Cells along a Hepatic Lineage. *Chem.-Biol. Interact.* **2011**, *190*, 62–72.

(6) Lee, K. D.; Kuo, T. K. C.; Whang-Peng, J.; Chung, Y. F.; Lin, C. T.; Chou, S. H.; Chen, J. R.; Chen, Y. P.; Lee, O. K. S. In Vitro Hepatic Differentiation of Human Mesenchymal Stem Cells. *Hepatology* **2004**, *40*, 1275–1284.

(7) Zhao, W.; Li, J. J.; Cao, D. Y.; Li, X.; Zhang, L. Y.; He, Y.; Yue, S. Q.; Wang, D. S.; Dou, K. F. Intravenous Injection of Mesenchymal Stem Cells Is Effective in Treating Liver Fibrosis. *World J. Gastroenterol.* **2012**, *18*, 1048–1058.

(8) Subramanian, K.; Owens, D. J.; O'Brien, T. D.; Verfaillie, C. M.; Hu, W. S. Enhanced Differentiation of Adult Bone Marrow-Derived Stem Cells to Liver Lineage in Aggregate Culture. *Tissue Eng., Part A* **2011**, *17*, 2331–2341.

(9) Parekkadan, B.; Milwid, J. M. Mesenchymal Stem Cells as Therapeutics. *Annu. Rev. Biomed. Eng.* **2010**, *12*, 87–117.

(10) Zhao, D. C.; Lei, J. X.; Chen, R.; Yu, W. H.; Zhang, X. M.; Li, S. N.; Xiang, P. Bone Marrow-Derived Mesenchymal Stem Cells Protect against Experimental Liver Fibrosis in Rats. *World J. Gastroenterol.* **2005**, *11*, 3431–3440.

(11) Piryaeei, A.; Valojerdi, M. R.; Shahsavani, M.; Baharvand, H. Differentiation of Bone Marrow-Derived Mesenchymal Stem Cells into Hepatocyte-like Cells on Nanofibers and Their Transplantation into a Carbon Tetrachloride-Induced Liver Fibrosis Model. *Stem Cell Rev.* **2011**, *7*, 103–118.

(12) Imamura, T.; Cui, L.; Teng, R.; Johkura, K.; Okouchi, Y.; Asanuma, K.; Ogiwara, N.; Sasaki, K. Embryonic Stem Cell-Derived Embryoid Bodies in Three-Dimensional Culture System form Hepatocyte-like Cells in Vitro and in Vivo. *Tissue Eng.* **2004**, *10*, 1716–1724.

(13) Cai, J.; Zhao, Y.; Liu, Y.; Ye, F.; Song, Z.; Qin, H.; Meng, S.; Chen, Y.; Zhou, R.; Song, X.; Guo, Y.; Ding, M.; Deng, H. Directed Differentiation of Human Embryonic Stem Cells into Functional Hepatic Cells. *Hepatology* **2007**, *45*, 1229–1239.

(14) Ong, S. Y.; Dai, H.; Leong, K. W. Inducing Hepatic Differentiation of Human Mesenchymal Stem Cells in Pellet Culture. *Biomaterials* **2006**, *27*, 4087–4097.

(15) Ryu, K. H.; Cho, K. A.; Park, H. S.; Kim, J. Y.; Woo, S. Y.; Jo, I.; Choi, Y. H.; Park, Y. M.; Jung, S. C.; Chung, S. M.; Choi, B. O.; Kim, H. S. Tonsil-Derived Mesenchymal Stromal Cells: Evaluation of Biologic, Immunologic and Genetic Factors for Successful Banking. *Cytherapy* **2012**, *14*, 1193–1202.

(16) Janjanin, S.; Djouad, F.; Shanti, R. M.; Baksh, D.; Gollapudi, K.; Prgomet, D.; Rackwitz, L.; Joshi, A. S.; Tuan, R. S. Human Palatine Tonsil: A New Potential Tissue Source of Multipotent Mesenchymal Progenitor Cells. *Arthritis Res. Ther.* **2008**, *10*, R83.

(17) Yu, L.; Ding, J. Injectable Hydrogels as Unique Biomedical Materials. *Chem. Soc. Rev.* **2008**, *37*, 1473–1481.

(18) Loh, X. J.; Li, J. Biodegradable Thermosensitive Copolymer Hydrogels for Drug Delivery. *Expert Opin. Ther. Pat.* **2007**, *17*, 965–977.

(19) Nagahama, K.; Ouchi, T.; Ohya, Y. Temperature-Induced Hydrogels through Self-Assembly of Cholesterol-Substituted Star PEG-b-PLLA Copolymers: An Injectable Scaffold for Tissue Engineering. *Adv. Funct. Mater.* **2008**, *18*, 1220–1231.

(20) He, C.; Kim, S. W.; Lee, D. S. In Situ Gelling Stimuli-Sensitive Block Copolymer Hydrogels for Drug Delivery. *J. Controlled Release* **2008**, *127*, 189–207.

(21) Yeon, B.; Park, M. H.; Moon, H. J.; Kim, S. J.; Cheon, Y. W.; Jeong, B. 3D Culture of Adipose-Tissue-Derived Stem Cells Mainly Leads to Chondrogenesis in Poly(ethylene glycol)-poly(L-alanine) Diblock Copolymer Thermogel. *Biomacromolecules* **2013**, *14*, 3256–3266.

(22) Park, M. H.; Choi, B. G.; Jeong, B. Complexation-Induced Biomimetic Long Range Fibrous Orientation in a Rigid-Flexible Block Copolymer Thermogel. *Adv. Funct. Mater.* **2012**, *22*, 5118–5125.

(23) Moon, H. J.; Ko, D. Y.; Park, M. H.; Joo, M. K.; Jeong, B. Temperature-Responsive Compounds as in Situ Gelling Biomedical Materials. *Chem. Soc. Rev.* **2012**, *41*, 4860–4883.

(24) Blanzas, A.; Verber, R.; Mykhaylyk, O. O.; Ryan, A. J.; Heath, J. Z.; Douglas, C. W. I.; Armes, S. P. Sterilizable Gels from Thermoresponsive Block Copolymer Worms. *J. Am. Chem. Soc.* **2012**, *134*, 9741–9748.

(25) Jeong, Y.; Joo, M. K.; Bahk, K. H.; Choi, Y. Y.; Kim, H. T.; Kim, W. K.; Lee, H. J.; Sohn, Y. S.; Jeong, B. Enzymatically Degradable Temperature-Sensitive Polypeptide as a New in-Situ Gelling Biomaterial. *J. Controlled Release* **2009**, *137*, 25–30.

(26) Choi, Y. Y.; Joo, M. K.; Sohn, Y. S.; Jeong, B. Significance of Secondary Structure in Nanostructure Formation and Thermosensitivity of Polypeptide Block Copolymers. *Soft Matter* **2008**, *4*, 2383–2387.

(27) Lee, M. J.; Jung, J.; Na, K. H.; Moon, J. S.; Lee, H. J.; Kim, J. H.; Kim, G. I.; Kwon, S. W.; Hwang, S. G.; Kim, G. J. Anti-Fibrotic Effect of Chorionic Plate-Derived Mesenchymal Stem Cells Isolated from Human Placenta in a Rat Model of CCl<sub>4</sub>-Injured Liver: Potential Application to the Treatment of Hepatic Diseases. *J. Cell. Biochem.* **2010**, *111*, 1453–1463.

(28) Ji, R.; Zhang, N.; You, N.; Li, Q.; Liu, W.; Jiang, N.; Liu, J.; Zhang, H.; Wang, D.; Tao, K.; Dou, K. The Differentiation of MSCs into Functional Hepatocyte-like Cells in a Liver Biomatrix Scaffold and Their Transplantation into Liver-Fibrotic Mice. *Biomaterials* **2012**, *33*, 8995–9008.

(29) Talens-Visconti, R.; Bonora, A.; Jover, R.; Mirabet, V.; Carbonell, F.; Castell, J. V.; Gomez-Lechon, M. J. Human Mesenchymal Stem Cells from Adipose Tissue: Differentiation into Hepatic Lineage. *Toxicol. in Vitro* **2007**, *21*, 324–329.

(30) Liu, T.; Zhang, S.; Chen, X.; Li, G.; Wang, Y. Hepatic Differentiation of Mouse Embryonic Stem Cells in Three-Dimensional Polymer Scaffolds. *Tissue Eng., Part A* **2010**, *16*, 1115–1122.

(31) Guo, Q.; Thomann, R.; Gronski, W.; Staneva, R.; Ivanova, R.; Stuhn, B. Nanostructures, Semicrystalline Morphology, and Nanoscale Confinement Effect on the Crystallization Kinetics in Self-Organized Block Copolymer/Thermoset Blends. *Macromolecules* **2003**, *36*, 3635–3645.

(32) Liu, Z.; Fan, Y.; Tian, M.; Wang, R.; Han, Y.; Wang, Y. Surfactant Selection Principle for Reducing Critical Micelle Concentration in Mixtures of Oppositely Charged Gemini Surfactants. *Langmuir* **2014**, *30*, 7968–7976.

(33) Wei, Y.; Wang, F.; Zhang, Z.; Ren, C.; Lin, Y. Micellization and Thermodynamic Study of 1-Alkyl-3-methylimidazolium Tetrafluoroborate Ionic Liquids in Aqueous Solution. *J. Mater. Chem. B* **2013**, *1*, 668–675.

(34) Domínguez, A.; Fernández, A.; González, N.; Iglesias, E.; Montenegro, L. Determination of Critical Micelle Concentration of Some Surfactants by Three Techniques. *J. Chem. Educ.* **1997**, *74*, 1227–1231.

(35) Qin, S.-Y.; Pei, Y.; Liu, X.-J.; Zhuo, R.-X.; Zhang, X.-Z. Hierarchical Self-Assembly of a  $\beta$ -Amyloid Peptide Derivative. *J. Mater. Chem. B* **2013**, *1*, 668–675.

(36) Liu, T.; Nace, V. M.; Chu, B. Self-Assembly of Mixed Amphiphilic Triblock Copolymers in Aqueous Solution. *Langmuir* **1999**, *15*, 3109–3117.

(37) Nagy, M.; Szollosi, L.; Keki, S.; Zsuga, M. Self-Assembly Study of Polydisperse Ethylene Oxide-Based Nonionic Surfactants. *Langmuir* **2007**, *23*, 1014–1017.

(38) Shimada, T.; Megley, K.; Tirrell, M.; Hotta, A. Fluid Mechanical Shear Induces Structural Transitions in Assembly of a Peptide–Lipid Conjugate. *Soft Matter* **2011**, *7*, 8856–8861.

(39) Kim, J. Y.; Park, M. H.; Joo, M. K.; Lee, S. Y.; Jeong, B. End Groups Adjust Molecular Nano-Assembly Pattern and Thermal Gelation of Polypeptide Block Copolymer Aqueous Solution. *Macromolecules* **2009**, *42*, 3147–3151.

- (40) Evans, D. W.; Moran, E. C.; Baptista, P. M.; Soker, S.; Sparks, J. L. Scale-Dependent Mechanical Properties of Native and Decellularized Liver Tissue. *Biomech. Model. Mechanobiol.* **2013**, *12*, 569–580.
- (41) Hwang, N. S.; Kim, M. S.; Sampattavanich, S.; Baek, J. H.; Zhang, Z.; Elisseff, J. Effects of Three-Dimensional Culture and Growth Factors on the Chondrogenic Differentiation of Murine Embryonic Stem Cells. *Stem Cells* **2006**, *24*, 284–291.
- (42) Campard, D.; Lysy, P. A.; Najimi, M.; Sokal, E. M. Native Umbilical Cord Matrix Stem Cells Express Hepatic Markers and Differentiate into Hepatocyte-like Cells. *Gastroenterology* **2008**, *134*, 833–848.
- (43) Lau, T. T.; Ho, L. W.; Wang, D. A. Hepatogenesis of Murine Induced Pluripotent Stem Cells in 3D Micro-Cavitary Hydrogel System for Liver Regeneration. *Biomaterials* **2013**, *34*, 6659–6669.
- (44) Hamazaki, T.; Iiboshi, Y.; Oka, M.; Papst, P. J.; Meacham, A. M.; Zon, L. I.; Terada, N. Hepatic Maturation in Differentiating Embryonic Stem Cells in Vitro. *FEBS Lett.* **2001**, *497*, 15–19.
- (45) Valva, P.; De Matteo, E.; Galoppo, M. C.; Gismondi, M. I.; Preciado, M. V. Apoptosis Markers Related to Pathogenesis of Pediatric Chronic Hepatitis C Virus Infection: M30 Mirrors the Severity of Steatosis. *J. Med. Virol.* **2010**, *82*, 949–957.
- (46) Sidhu, J. S.; Liu, F.; Omiecinski, C. J. Phenobarbital Responsiveness as a Uniquely Sensitive Indicator of Hepatocyte Differentiation Status: Requirement of Dexamethasone and Extracellular Matrix in Establishing the Functional Integrity of Cultured Primary Rat Hepatocytes. *Exp. Cell Res.* **2004**, *292*, 252–264.
- (47) Clotman, F.; Lemaigre, F. P. Control of Hepatic Differentiation by Activin/TGF $\beta$  Signaling. *Cell Cycle* **2006**, *5*, 168–171.
- (48) Cascio, S.; Zaret, K. S. Hepatocyte Differentiation Initiates during Endodermal-Mesenchymal Interactions Prior to Liver Formation. *Development* **1991**, *113*, 217–225.
- (49) Shiojiri, N. Enzyme- and Immunocytochemical Analyses of the Differentiation of Liver Cells in the Prenatal Mouse. *J. Embryol. Exp. Morphol.* **1981**, *62*, 139–152.
- (50) Hong, S. H.; Gang, E. J.; Jeong, J. A.; Ahn, C.; Hwang, S. H.; Yang, I. H.; Park, H. K.; Han, H.; Kim, H. In Vitro Differentiation of Human Umbilical Cord Blood-Derived Mesenchymal Stem Cells into Hepatocyte-like Cells. *Biochem. Biophys. Res. Commun.* **2005**, *330*, 1153–1161.
- (51) Chivu, M.; Dima, S. O.; Stancu, C. I.; Dobrea, C.; Uscatescu, V.; Necula, L. G.; Bleotu, C.; Tanase, C.; Albuiescu, R.; Ardeleanu, C.; Popescu, I. In Vitro Hepatic Differentiation of Human Bone Marrow Mesenchymal Stem Cells under Differential Exposure to Liver-Specific Factors. *Transl. Res.* **2009**, *154*, 122–132.
- (52) Yamada, T.; Yoshikawa, M.; Kanda, S.; Kato, Y.; Nakajima, Y.; Ishizaka, S.; Tsunoda, Y. In Vitro Differentiation of Embryonic Stem Cells into Hepatocyte-like Cells Identified by Cellular Uptake of Indocyanine Green. *Stem Cells* **2002**, *20*, 146–154.
- (53) Iwamuro, M.; Komaki, T.; Kubota, Y.; Seita, M.; Kawamoto, H.; Yuasa, T.; Shahid, J. M.; Hassan, R. A. R. A.; Hassan, W. A. R. A.; Nakai, S.; Nishikawa, Y.; Kondo, E.; Yamamoto, K.; Fox, I. J.; Kobayashi, N. Hepatic Differentiation of Mouse iPS Cells in Vitro. *Cell Transplant.* **2010**, *19*, 841–847.
- (54) Soto-Gutierrez, A.; Kobayashi, N.; Rivas-Carrillo, J. D.; Navarro-Alvarez, N.; Zhao, D. B.; Okitsu, T.; Noguchi, H.; Basma, H.; Tabata, Y.; Chen, Y.; Tanaka, K.; Narushima, M.; Miki, A.; Ueda, T.; Jun, H. S.; Yoon, J. W.; Lebkowski, J.; Tanaka, N.; Fox, I. J. Reversal of Mouse Hepatic Failure Using an Implanted Liver-Assist Device Containing ES Cell-Derived Hepatocytes. *Nat. Biotechnol.* **2006**, *24*, 1412–1419.
- (55) Mizumoto, H.; Aoki, K.; Nakazawa, K.; Ijima, H.; Funatsu, K.; Kajiwara, T. Hepatic Differentiation of Embryonic Stem Cells in HF/Organoid Culture. *Transplant. Proc.* **2008**, *40*, 611–613.
- (56) Levenberg, S.; Huang, N. F.; Lavik, E.; Rogers, A. B.; Itskovitz-Eldor, J.; Langer, R. Differentiation of Human Embryonic Stem Cells on Three-Dimensional Polymer Scaffolds. *Proc. Natl. Acad. Sci. U.S.A.* **2003**, *100*, 12741–12746.
- (57) Kazemnejad, S.; Allameh, A.; Soleimani, M.; Gharehbaghian, A.; Mohammadi, Y.; Amirzadeh, N.; Jazayeri, M. Biochemical and Molecular Characterization of Hepatocyte-like Cells Derived from Human Bone Marrow Mesenchymal Stem Cells on a Novel Three-Dimensional Biocompatible Nanofibrous Scaffold. *J. Gastroenterol. Hepatol.* **2009**, *24*, 278–287.
- (58) Lin, N.; Lin, J.; Bo, L.; Weidong, P.; Chen, S.; Xu, R. Differentiation of Bone Marrow-Derived Mesenchymal Stem Cells into Hepatocyte-like Cells in an Alginate Scaffold. *Cell Proliferation* **2010**, *43*, 427–434.
- (59) Parashurama, N.; Nahmias, Y.; Cho, C. H.; Van Poll, D.; Tilles, A. W.; Berthiaume, F.; Yarmush, M. L. Activin Alters the Kinetics of Endoderm Induction in Embryonic Stem Cells Cultured on Collagen Gels. *Stem Cells* **2008**, *26*, 474–484.
- (60) Snykers, S.; Vanhaecke, T.; Papeleu, P.; Lutun, A.; Jiang, Y. H.; Vander Heyden, Y.; Verfaillie, C.; Rogiers, V. Sequential Exposure to Cytokines Reflecting Embryogenesis: The Key for in Vitro Differentiation of Adult Bone Marrow Stem Cells into Functional Hepatocyte-like Cells. *Toxicol. Sci.* **2006**, *94*, 330–341.
- (61) Kinoshita, T.; Miyajima, A. Cytokine Regulation of Liver Development. *Biochim. Biophys. Acta* **2002**, *1592*, 303–312.